30
Enantioselective Hydrogenation of Unfunctionalized Alkenes

Andreas Pfaltz and Sharon Bell

30.1
Introduction

Enantioselective hydrogenation of functionalized alkenes is a well-developed field. A wide variety of rhodium and ruthenium catalysts and substrates are available for this purpose (see Chapters 23 to 28), and the reaction is widely used as a common synthetic tool in both academia and industry.

Unfunctionalized alkenes have posed more of a problem, as they have no polar moiety which can coordinate to the catalyst. Such an additional metal binding site next to the C=C bond has proven to be crucial for directing coordination to the catalyst and, therefore, rhodium and ruthenium complexes, which are highly selective for functionalized alkenes, generally provide only low enantioselectivity for this class of substrates.

Initially, progress in this area was hampered by the lack of suitable analytical methods for chiral hydrocarbons. Early studies relied on optical rotation to determine enantiomeric excess (ee) values, but with the development of chiral gas chromatography (GC) and high-performance liquid chromatography (HPLC) columns, chromatographic methods have become more common.

Aided by these developments, the past five years has seen a rapid growth in this area. A breakthrough was the introduction of iridium catalysts with chiral P,N ligands. A large number of new P,N and other ligands have been synthesized and applied to the hydrogenation of unfunctionalized alkenes. This chapter details the catalysts, conditions and substrates used in the enantiomeric hydrogenation of unfunctionalized alkenes.

The Handbook of Homogeneous Hydrogenation.
Edited by J.G. de Vries and C.J. Elsevier

ISBN: 978-3-527-31161-3

30.2
Terminal Alkenes

30.2.1
2-Aryl-1-Butenes

The enantioselective hydrogenation of terminal 1,1-disubstituted olefins presents a particular challenge. Enantioface differentiation in the compounds relies on the different interactions of the catalyst with the two substituents which, as in the case of **1** and **2** (Fig. 30.1), are sterically quite similar.

Initially, research focused on the use of C_2-symmetric rhodium and ruthenium-phosphine and phosphinite complexes: a rhodium–phosphine complex **3** (Fig. 30.2) was used in the first reported enantioselective hydrogenation of substrate **1** (Table 30.1, entry 1) [1].

With most rhodium and ruthenium catalysts **4** and **5** (Fig. 30.2), only low enantioselectivities were obtained (Table 30.1, entries 1–6) [2–6]. However, good results were reported by Noyori and coworkers, who used DuPHOS with potassium *tert*-butoxide activation to hydrogenate substrate **1** in 86% ee (Table 30.1, entry 6) [6], as well as hydrogenating a range of other 1,1-disubstituted alkenes (see Section 30.2.2).

However, the best-researched group of catalysts for these substrates is the metallocenes (Fig. 30.3; Table 30.1, entries 7–13) [7–14]. The highest ee-value was obtained with the chiral samarium metallocene **10a**. Hydrogenation of **1** at –78 °C gave 2-phenylbutane in 96% ee (Table 30.1, entry 12) [12]. Turnover frequencies (TOFs) as high as 1210 h^{-1} have been recorded for these catalysts [14]. Catalyst **10b**, the titanocene analogue of **10a**, has been synthesized and used to hydrogenate **1** in 60% ee (Table 30.1, entry 13) [13].

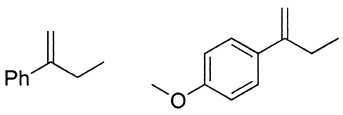

1 **2**

Fig. 30.1 Alkenes discussed in Section 30.2.1.

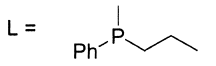

3

4

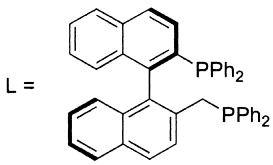

5

$[Rh(1,5\text{-hexadiene})L_2]^+Cl^-$ $[Rh(1,5\text{-hexadiene})L]^+Cl^-$ $[Rh(COD)L]^+Cl$

Fig. 30.2 Rhodium catalysts **3**, **4** and **5**.

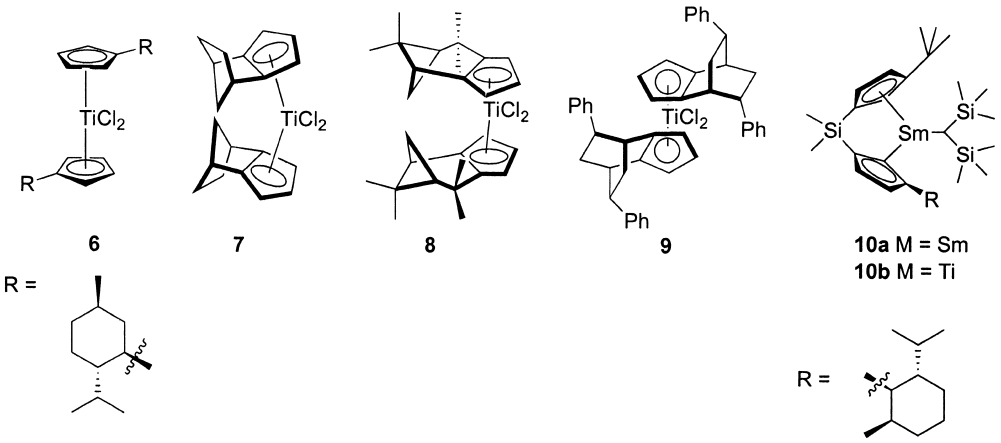

Fig. 30.3 Selected catalysts for the hydrogenation of substrate **1**.

More recently, Ir-JM-Phos **11** (Fig. 30.4) was used to hydrogenate **1** in a moderate 40% ee (Table 30.1, entry 14) [15]. This catalyst was found to be more selective in the hydrogenation of trisubstituted alkenes (see Section 30.3).

Substrate **2** has also been used as a test substrate: HPLC separation methods exist for **2**, while ee-value determination of **1** is more difficult [6, 17]. Reflecting the general recent interest in the hydrogenation of unfunctionalized olefins, the past few years have seen the publication of a number of results for this substrate [15, 18–26]. The highest enantioselectivities were achieved using catalysts **12b** [22] and **14a** [26].

Pressure effects have been found to have a significant effect on the enantioselectivity of hydrogenation of terminal olefins with ThrePHOX catalysts, in contrast to trisubstituted olefins [17, 25]. For example, in the hydrogenation of **2** with catalyst **12b**, 94% ee was obtained at 1 bar H_2, compared to 58% ee at 50 bar H_2 (Table 30.2).

The ThrePHOX catalyst was also used to hydrogenate a wider range of 2-aryl-1-butenes. Substrates **15–18**, **20** and **21** (Fig. 30.6) were hydrogenated in high yield and ee (Table 30.3).

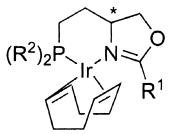

11a R^1 = ^{t}Bu R^2 = Ph

11b R^1 = Bn R^2 = *o*-tol

11c R^1 = *t*-Bu R^2 = *o*-tol

Fig. 30.4 Catalyst **11**.

Table 30.1 Hydrogenation of substrate **1**.

Entry	Catalyst	Loading [mol%]	Solvent	Temp. [°C]	Pressure [bar]	ee [%]	TOF [h^{-1}] (TON)[a]	Reference
1	**3**	0.5	Benzene	r.t.	1	8 (*S*)		1
2	**4**			50	50	33 (*R*)		2
3	Ru–DIOP	0.1	No solvent	20	100	1.9 (*S*)		3
4	BINAP	1.5	DCM	30	25	29 (*S*)	4	4
5	**5**	1	Benzene/ methanol	30	25	65 (*R*)	1	5
6	DuPHOS + *t*BuOK	0.5	2-Propanol	r.t.	8	74 (*R*)	13 (200)	6
7	**6**	1	Toluene	20	1	11.2[b] (*S*)		7
8	**6**	1	Hexane/ THF	5	1	28 (*S*)		8
9	**7**			–20		27[b] (*R*)		9
10	**8**	0.02–0.04	Toluene	r.t.	1	69 (*S*)		10
11	**9**	1	Toluene	–75	1	77[b] (*R*)	10	11
12	**10a**	0.2–1		–78		96 (*S*)	(500)	12
13	**10b**	1	Hexane/ THF	20	1	48 (*S*)	2 (100)	14
14	**11**	0.3	DCM	25	50	40 (*R*)	165	15

a) TOF data given where available; TON data given where reactions were complete after a standard reaction time, or where no time data were available.

b) Values corrected from the original papers, where ee calculations were based on an incorrect $[\alpha]_D$ value for 2-phenylbutane (22.7 rather than 28.4 [16]).

The DuPHOS/potassium *tert*-butoxide system was also used to hydrogenate these substrates, in addition to substrates **19** and **22** (Fig. 30.6; Table 30.4) [6]. Under normal conditions, ruthenium–diphosphine catalysts are known to be unreactive with styrenes: however, in the presence of potassium *tert*-butoxide, the substrates **15–22** were hydrogenated with high conversion.

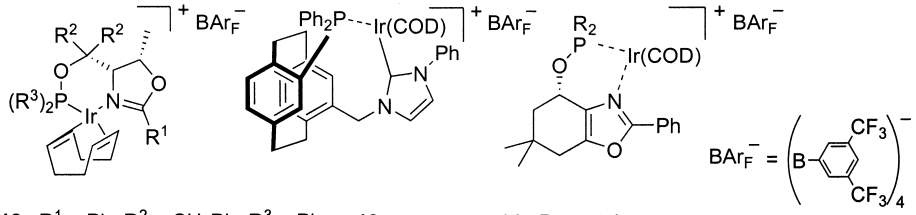

12a R^1 = Ph, R^2 = CH_2Ph, R^3 = Ph **13a**
12b R^1 = Ph, R^2 = CH_2Ph, R^3 = Cy
12c R^1 = 3,5-(tBu)$_2C_6H_3$, R^2 = CH_2Ph, R^3 = Ph
12d R^1 = 3,5-$Me_2C_6H_3$, R^2 = CH_2Ph, R^3 = Ph

14a R = *o*-tol
14b R = Ph
14c R = 3,5-$Me_2C_6H_3$

Fig. 30.5 Selected catalysts for the hydrogenation of substrate **2**.

Table 30.2 Most selective hydrogenations of substrate **2**.

Entry	Catalyst	Loading [mol%]	Solvent	Temp. [°C]	Pressure [bar]	ee [%]	TOF [h^{-1}] (TON)[a]	Reference
1	**12a**	1	DCM	0	1	89 (*R*)	50 (100)	22
2	**12b**	1	DCM	25	1	94	200 (100)	25
3	**13a**	1	DCM	25	1	79 (*S*)	(100)	23
4	**14a**	0.5	DCM	r.t.	50	97 (*S*)	100 (200)	26

a) TON data given where reactions were complete after a standard reaction time, or where no time data were available.

Table 30.3 Hydrogenation of substrates **15**–**18**, **20** and **21** with ThrePHOX catalyst **12b**.

Substrate	ee [%]	Conversion [%]	Pressure [bar]	Catalyst loading [mol%]	TOF [h^{-1}] (TON)[a]
15	91	>99	1	1	200 (100)
16	88	>99	1	1	200 (100)
17	89	>99	1	1	200 (100)
18	93	>99	1	1	200 (100)
20	92	>99	1	1	200 (100)
21	94	>99	1	1	200 (100)

a) All reactions were complete after standard reaction time of 30 min: the calculated TOF is a lower limit of the true TOF.

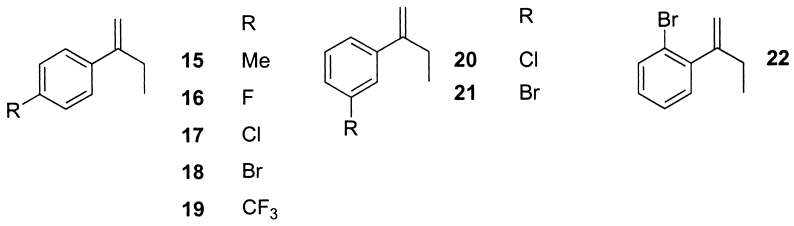

Fig. 30.6 Substrates **15**–**22**.

Table 30.4 Hydrogenation of substrates **15**–**22** with $RuCl_2[(R,R)\text{-MeDuPHOS}](DMF)_n$.[a)]

Substrate	ee [%]	Absolute configuration	Conversion [%]	Catalyst loading [mol%]	TOF [h^{-1}] (TON)[b)]
15	87	*R*	87	0.3	20
16	82	*R*	97	0.15	40
17	85	*R*	94	0.07	80
18	83	*R*	100	0.15	40 (660)
19	81	*R*	99.5	0.04	160
20	89	*R*	87	0.2	30
21	86	*R*	100	0.2	30 (520)
22	69	*R*	33	0.26	8

a) Hydrogenations carried out in 2-propanol at 30 °C using 8 bar H_2.

b) TON data given where reactions were complete after a standard reaction time, or where no time data were available.

30.2.2 Other Terminal Alkenes

A range of other terminal alkenes has been hydrogenated with ruthenium–diphosphine catalysts. The first set of substrates (Fig. 30.7; Table 30.5) was hydrogenated with Ru–BINAP in dichloromethane (DCM) at 30 °C. Products of double bond migration were also detected [5].

The modified BINAP catalyst **5** has been used for the hydrogenation of a number of analogues of substrate **1** (substrates **32**–**35**, Fig. 30.8; Table 30.6), though again, enantioselectivities were modest [4]. Substrate **31** has also been hydrogenated with a ruthenium–BINAP-hydride cluster with low selectivity (11% ee) [27].

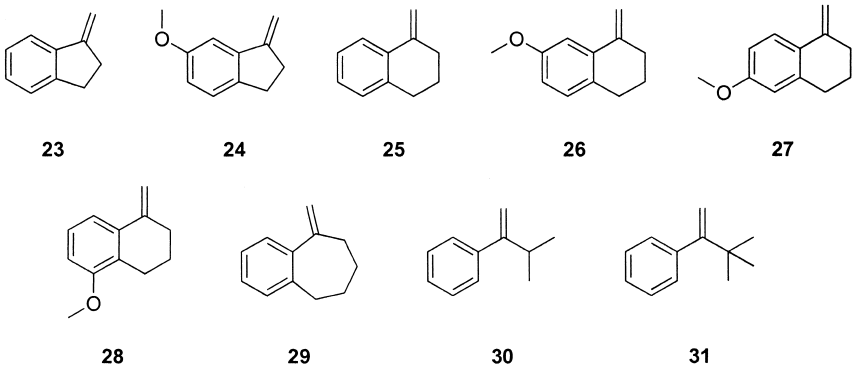

Fig. 30.7 Substrates **23**–**31**.

Table 30.5 Hydrogenation of substrates **23**–**31** with $[Rh(BINAP)(COD)]^+X^-$.[a)]

Substrate	ee [%]	Absolute configuration	Conversion [%]	Pressure [bar]	Catalyst loading [mol%]	TOF [h^{-1}]
23[b)]	78	*S*	100	100	4	1
24[b)]	45	–	100	100	4	1
25	80	*S*	81	25	1.5	15
26	71	(+)	85	25	1.5	16
27[b)]	75	–	100	100	4	0.6
28[b)]	61	(+)	100	100	4	0.6
29	44	(–)	56	25	1.5	1.6
30	35	*R*	100	25	1.5	0.8
31	40	–	87	25	1.5	1

a) Hydrogenations carried out in DCM at 30 °C.
b) Isomerization products also detected.

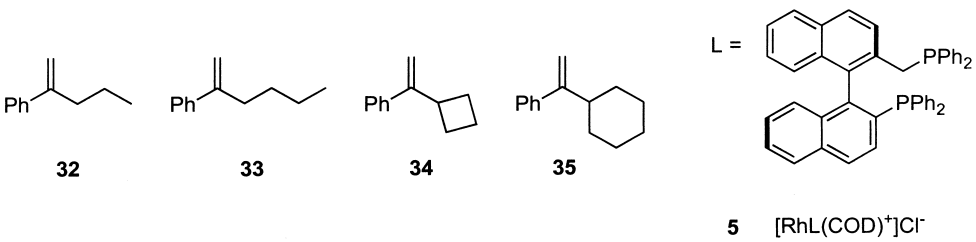

Fig. 30.8 Substrates **32**–**35** and catalyst **5**.

Table 30.6 Hydrogenation of substrates **30**–**35** with catalyst **5**.[a)]

Substrate	ee [%]	Absolute configuration	Conversion [%]	TOF [h^{-1}] (TON)[b)]
30	17	*R*	100	4 (100)
31	31	*R*	75	3
32	77	*R*	100	2
33	55	*R*	100	4 (100)
34	16	(–)	100	4 (100)
35	2	*R*	100	2

a) Hydrogenations performed in 1:1 benzene:methanol at 30 °C using 25 bar H_2 and 1 mol% catalyst.
b) TON data given where reactions were complete after a standard reaction time, or where no time data were available.

30.3 Trisubstituted Alkenes

30.3.1 Introduction

Substrates **36** to **40** (Fig. 30.9) have become standard test substrates, and many catalysts have been evaluated with this set of alkenes. For that reason the hydrogenation of these test substrates is discussed in one section. Some catalysts have also been used to hydrogenate a wider variety of alkenes (see Section 30.3.2).

Initially, the benchmark for the enantioselective hydrogenation of trisubstituted unfunctionalized alkenes was set very high, with the titanocene catalyst **41** (Fig. 30.10) being used to hydrogenate test substrates **36**, **38** and **40**, as well as some others (see Section 30.3.2) in very high selectivity [28]. However, the catalysts were not very active, requiring high catalyst loadings (4 mol%) and long reaction times. Phosphino-oxazoline-derived iridium catalysts (Ir–PHOX, **42**; Fig. 30.10), which were introduced later, gave very high ee-values with diaryl alkenes **36** and **37** and moderate to good enantioselectivities with substrates **38**, **36**, and **39** [29, 30]. The turnover number (TON) and TOF were clearly superior compared with the titanocene **41**. Substrate **43** was also hydrogenated with this catalyst in 95% ee.

Subsequently, further investigations were focused on this catalyst class.

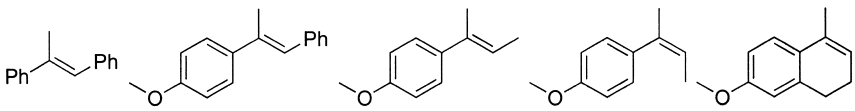

36 **37** **38** **39** **40**

Fig. 30.9 Trisubstituted alkenes used as test substrates.

30.3.2 Ir Catalysts

As discussed below, Ir complexes derived from chiral P,N ligands have become the catalysts of choice for the enantiomeric hydrogenation of unfunctionalized trisubstituted olefins. Therefore, the most important characteristics of these catalysts are briefly summarized here [30–32].

The catalyst precursors (cationic Ir–COD complexes with weakly coordinating anions such as BAr_F) are air- and moisture-stable, and are therefore easy to handle. It is possible to store them for several months under air. Two of the most versatile catalysts (ThrePHOX catalysts, **12a** and **12b**) recently became commercially available [33].

The catalysts are highly reactive: maximum TOFs of $>5000\ h^{-1}$ at 277 K were measured for the hydrogenation of substrate **2** with catalysts of type **42**. The reaction is mass transfer-limited at room temperature and, therefore, a value of $5000\ h^{-1}$ represents a lower limit for the possible maximum TOF [31]. Full conversion was achieved with catalyst loadings as low as 0.01 mol% (substrate **2**, catalyst **12a**).

Reactions are typically run at 10 to 100 bar H_2, though pressure has a minimal effect on enantioselectivity.

Common solvents used are DCM, 1,2-dichloroethane, and toluene. More strongly coordinating solvents such as tetrahydrofuran (THF), acetonitrile or alcohols deactivate the catalyst.

The anion plays a crucial role. BAr_F and other bulky fluorinated tetra-arylborates or tetraalkoxyaluminates are the most suitable anions. Hexafluorophosphate-containing catalysts display high reactivity in the initial phase of the reaction, but suffer deactivation before the reaction reaches completion. Tetrafluoroborate, triflate or other more strongly coordinating anions inhibit the catalyst.

In contrast to the hydrogenation of imines, where addition of acids and/or iodine often has a beneficial effect, here additives of this type were found to deactivate the catalyst.

30.3.3 Standard Test Substrates

The promising results obtained with Ir–PHOX complexes prompted an extensive search for related, more selective catalysts with broader substrate scope.

The diamine and TADDOL-derived catalysts **44** were tested on substrates **36**–**39**, giving good enantioselectivities; however, high catalyst loadings of 4 mol% were required for full conversion [34].

SimplePHOX complex **45** (Fig. 30.10) was used to hydrogenate substrates **36** and **38**–**40**, and proved to be one of the most selective catalysts for the hydrogenation of substrate **40** [24].

A new group of PHOX catalysts was developed, based on the attachment of the oxazoline at the 2-position rather than the 5-position as in the original

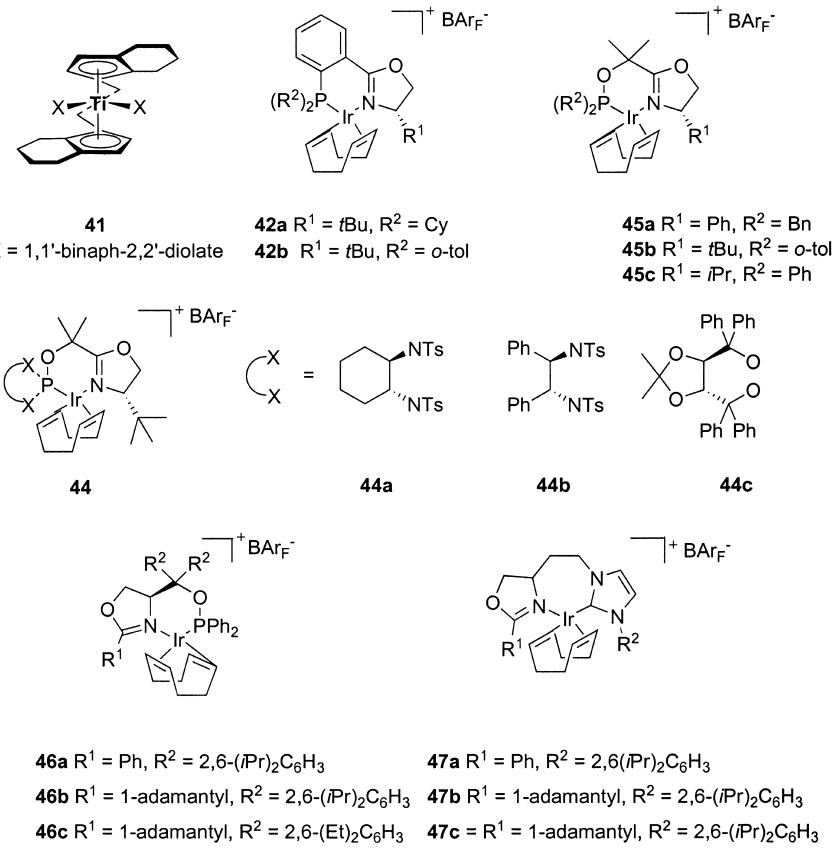

Fig. 30.10 Selected catalysts for the hydrogenation of trisubstituted alkenes.

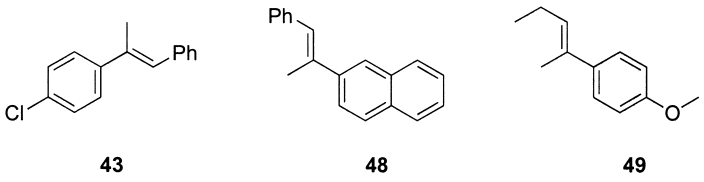

Fig. 30.11 Substrates **43**, **48** and **49**.

PHOX catalysts. While the first generation of these catalysts (SerPHOX **46**, Fig. 30.10) hydrogenated substrates **36** and **38–40** in good yield and ee [19], significant progress was made with the second generation of catalysts [22]. With an additional chiral center, ThrePHOX catalysts **12** (Fig. 30.5) gave very high enantioselectivities, particularly for substrates **38** (Table 30.9, entry 7) and **39** (Table 30.10, entry 7). Complexes **12** are also efficient catalysts for the hydrogenation of 1,1-disubstituted substrates (see Section 30.2.1).

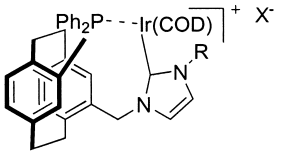

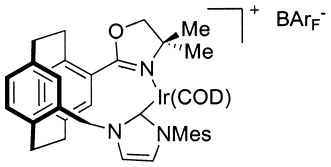

13a R = Ph, X^- = BAr_F^-
13b R = 2,4,6-Me_3Ph, X^- = BAr_F^-
13c R = 2,6-*i*-Pr_2Ph, X^- = BAr_F^-
13d R = 2,4,6-Me_3Ph, X^- = PF_6^-

50

Fig. 30.12 Catalysts **13** and **50**.

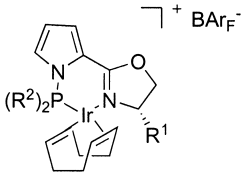

51 [37]
R^1 = *i*Pr, *t*Bu; R^2 = aryl, Cy

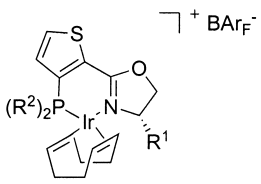

52a [38]
R^1 = *i*Pr, *t*Bu; R^2 = aryl, Cy

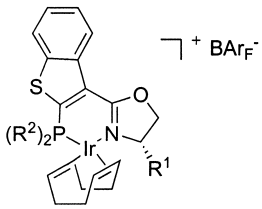

52b [38]
R^1 = *i*Pr, *t*Bu; R^2 = aryl

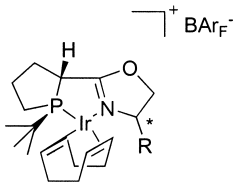

R = *i*Pr, *t*Bu, Ph, Bn, *i*Bu
54 [39]

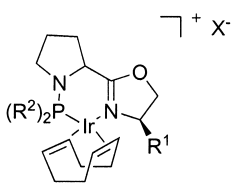

R = aryl, X = BAr_F, PF_6
55 [40]

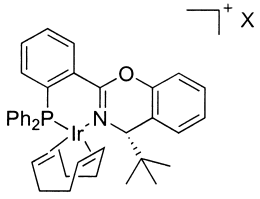

56a X = BAr_F^- [18]
56b X = PF_6^-

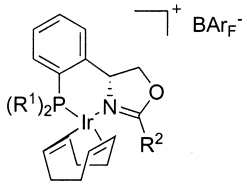

R^1 = Ph, Cy;
R^2 = bulky aryl, alkyl

57 [41]

Fig. 30.13 Catalysts **51**–**57**.

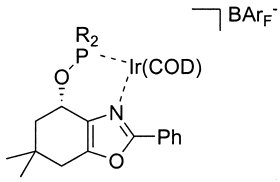

Fig. 30.14 Oxazole–phosphinite complex **14**.

14a R = *o*-tol
14b R = Ph
14c R = 3,5-Me$_2$Ph

The structurally related JM-Phos catalyst **11** (Fig. 30.10) gave generally lower selectivity for substrates **36–40** [15]. Deuteration studies using D_2 with these catalysts showed substantial deuterium incorporation into the allylic positions of substrates **39** and **2**. Deuterium incorporation has also been observed with Ir–PHOX catalysts [35], which implies that reversible H abstraction at the allylic position occurs during the hydrogenation reaction.

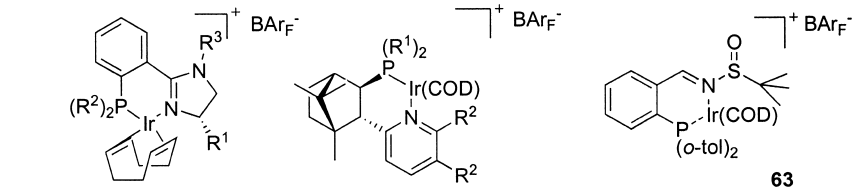

58a R^1 = *t*Bu, R^2 = *o*-tol, R^3 = Ph
58b R^1 = *t*Bu, R^2 = *o*-tol, R^3 = Bn

59a R^1 = Ph, R^2 = H
59b R^1 = Ph, R^2 = -CH_2CH=$CHCH_2$-

63

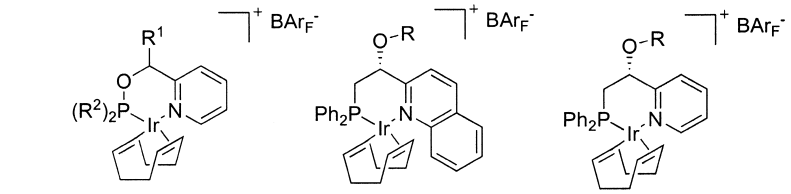

60

a R^1 = *t*Bu, R^2 = *t*Bu (*S*)
b R^1 = Ph, R^2 = Ph
c R^1 = *t*Bu, R^2 = Ph (*S*)
d R^1 = *t*Bu, R^2 = *o*-tol (*R*)
e R^1 = *t*Bu, R^2 = Cy (*S*)
f R^1 = trityl, R^2 = Ph (*R*)

61

a R = Si(*t*Bu)Me$_2$
b R = Si(*i*Pr)$_3$
c R = Si(*t*Bu)Ph$_2$

62

a R = Si(*t*Bu)Me$_2$
b R = Si(*i*Pr)$_3$
c R = Si(*t*Bu)Ph$_2$

Fig. 30.15 Catalysts **58–63**.

Table 30.7 Hydrogenation of substrate **36**.

Entry	Catalyst	Loading [mol%]	Solvent	Temp. [°C]	Pressure [bar]	ee [%]	TOF [h^{-1}] (TON)[a)]	Reference
1	**41**	5	THF	65	5	>99 (*S*)	2	28
2	**42a**	1	DCM	25	50	99 (*R*)	50 (100)	30
3	**44a**	4	DCM	r.t.	100	94 (*R*)	2	34
4	**47a**	0.2–0.6	DCM	25	50	98 (*S*)	250	21
5	**45a**	1	DCM	r.t.	50	99 (*R*)	50 (100)	24
6	**46a**	0.4	DCM	23	50	98 (*R*)	125 (250)	19
7	**12a**	0.02	DCM	r.t.	50	99 (*R*)	2500 (5000)	22
8	**11b**	0.2	DCM	25	50	95 (*S*)	250	15
9	**58a**	1	DCM	r.t.	50	94 (*R*)	50 (100)	42
10	**14b**	0.5	DCM	r.t.	30	>99 (*S*)	100 (200)	26
11	**59a**	0.5	toluene	25	50	95 (*S*)	8 (100)	43
12	**50**	1	DCM	25	50	28 (*R*)		36
13	**13a**	1	DCM	25	50	82 (*R*)	4	23
14	**60a**	1	DCM	r.t.	50	97 (*R*)	50 (100)	44
15	**63**	5	DCM	r.t.	50	94 (*R*)	20	45

a) TON data given where reactions were complete after a standard reaction time, or where no time data were available.

In addition to P,N ligands, the carbenoid-oxazoline catalysts **47** (Fig. 30.10) were used to hydrogenate test substrates **36**–**39**, as well as substrates **48** and **49**, which were hydrogenated in 93% ee and 84% ee, respectively [21]. These catalysts were also used to hydrogenate 1,1-disubstituted alkenes (see Section 30.2.1).

In recent years, many related ligands have been produced. Bolm and co-workers have produced new carbenoid catalysts **13** and **50** (Fig. 30.12) based on a paracyclophane backbone [23, 36]. To date, however, enantioselectivities have been modest with these catalysts.

Table 30.8 Hydrogenation of substrate **37**.

Entry	Catalyst	Loading [mol%]	Solvent	Temp. [°C]	Pressure [bar]	ee [%]	TOF [h^{-1}] (TON)[a)]	Reference
1	**42a**	1	DCM	25	50	99 (*R*)	50 (100)	30
2	**44b**	4	DCM	r.t.	100	92 (*R*)	7	34
3	**47a**	0.6	DCM	25	50	97 (*S*)	80	21
4	**11c**	0.2	DCM	–5	70	94 (*S*)	150	15
5	**59b**	1	toluene	25	50	95 (*S*)	40	43

a) TON data given where reactions were complete after a standard reaction time, or where no time data were available.

Table 30.9 Hydrogenation of substrate **38**.

Entry	Catalyst	Loading [mol%]	Solvent	Temp. [°C]	Pressure [bar]	ee [%]	TOF [h^{-1}] (TON)[a]	Reference
1	**41**	5	THF	65	133	95 (*R*)	0.3	28
2	**42b**	0.1	DCM	r.t.	50	61 (*R*)	(330)	29
3	**44b**	4	DCM	r.t.	100	85 (*R*)	10 (25)	34
4	**47a**	0.6	DCM	25	50	91 (*S*)	80 (165)	21
5	**45b**	1	DCM	r.t.	50	91 (*R*)	50 (100)	24
6	**46b**	0.1	DCM	23	50	96 (*R*)	500 (1000)	19
7	**12c**	0.1	DCM	r.t.	50	99 (*R*)	500 (1000)	22
8	**11a**	0.6	DCM	25	50	80 (*S*)	75	15
9	**14a**	0.5	DCM	r.t.	50	96 (*S*)	100 (200)	26
10	**58b**	1	DCM	r.t.	50	90 (*R*)	50 (100)	42
11	**13a**	1	DCM	25	50	37 (*R*)	(100)	23
12	**60b**	1	DCM	r.t.	50	87	(100)	44

a) TON data given where reactions were complete after a standard reaction time, or where no time data were available.

A number of ligands have been prepared in which the PHOX aryl bridge has been replaced by heterocyclic rings, as shown in Figure 30.13. A phosphino-oxazoline complex **56** and a PHOX analogue **57**, in which the phenyl bridge is attached to C(5) of the oxazoline ring, have also been reported. None of these catalysts had any particular advantages compared to the best PHOX or SerPHOX/

Table 30.10 Hydrogenation of substrate **39**.

Entry	Catalyst	Loading [mol%]	Solvent	Temp. [°C]	Pressure [bar]	ee [%]	TOF [h^{-1}] (TON)[a]	Reference
1	**41**	5	THF	65	133	31	0.1	28
2	**45c**	1	DCM	r.t.	50	89 (*R*)	50 (100)	24
3	**42b**	1	DCM	r.t.	50	42	(97)	29
4	**44c**	4	DCM	r.t.	100	90 (*S*)	10 (25)	34
5	**47a**	0.6	DCM	25	50	80 (*R*)	50	21
6	**49c**	0.4	DCM	23	50	85 (*S*)	125 (250)	19
7	**12d**	1	DCM	r.t.	50	92 (*S*)	50 (100)	22
8	**11a**	0.6	DCM	25	50	75 (*R*)	60	15
9	**58a**	1	DCM	r.t.	50	88 (*S*)	50 (100)	42
10	**13a**	1	DCM	25	50	79 (*R*)	(100)	23
11	**60b**	1	DCM	r.t.	50	90	(100)	44

a) TON data given where reactions were complete after a standard reaction time, or where no time data were available.

Table 30.11 Hydrogenation of substrate **40**.

Entry	Catalyst	Loading [mol%]	Solvent	Temp. [°C]	Pressure [bar]	ee [%]	TOF [h^{-1}] (TON)[a)]	Reference
1	**41**	5	THF	65	120	93	0.1	28
2	**45b**	0.2	DCM	r.t.	50	95 (*S*)	50 (100)	24
3	**46c**	0.5	DCM	23	50	85 (*S*)	100 (200)	19
4	**12a**	0.1	DCM	r.t.	50	85 (*S*)	50 (100)	22
5	**14a**	0.5	DCM	r.t.	50	94 (*R*)	100 (200)	26
6	**58a**	1	DCM	r.t.	50	91 (*S*)	50 (100)	42

a) TON data given where reactions were complete after a standard reaction time, or where no time data were available.

ThrePHOX complexes. The phospholane **54** and catalyst **57**, however, gave promising results for the hydrogenation of *α,β*-unsaturated carboxylic esters.

The oxazole–phosphinite complexes **14** (Fig. 30.14) proved to be highly selective catalysts, comparable to the best catalysts developed so far (see entries in Tables 30.9 and 30.11–30.13) [26].

Catalyst **58**, in which the oxazoline ring has been replaced with an imidazoline, gave ee-values in the low 90% region for substrates **36** and **38–40** [42]. However, for certain substrates (see Section 30.5), replacement of the oxazoline by an imidazoline has resulted in significantly higher enantioselectivity. Recently, a number of pyridine- and quinoline-derived iridium complexes **59–62** have been developed, which gave promising enantioselectivities with substrates **36–39** [43, 44]. However, these catalysts cannot yet compete with the most efficient oxazoline-based complexes and complex **14**.

The sulfinyl imine catalyst **63**, which has a stereogenic sulfur atom, hydrogenated substrate **36** in 94% ee; however, high catalyst loadings were used [45].

The full results for substrates **36–40** are detailed in Tables 30.7 to 30.11.

In summary, the most efficient catalysts for substrates **36–40** are the SerPHOX and ThrePHOX complexes **46** and **12**, as well as the recently reported oxazole–phosphinite complexes **14**.

30.3.4 Other Substrates

The titanocene catalyst **41** was used to hydrogenate a range of aryl-substituted alkenes (Fig. 30.16, Table 30.12) [28].

Styrene derivatives **68–71** (Fig. 30.17; Table 30.13) were hydrogenated with moderate to high selectivity using carbene complexes **13a** and **13b** [20].

Recently, a breakthrough in the hydrogenation of unfunctionalized olefins was made [51]. For the first time, high enantioselectivities with purely alkyl-substituted alkenes such as **72–74** could be achieved using pyridine–phosphinite catalysts **75** and **76**.

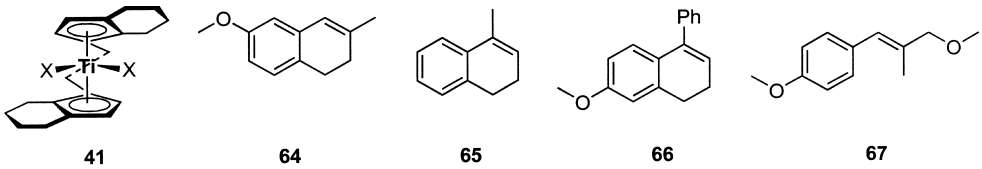

41 **64** **65** **66** **67**

X_2 = 1,1'-binaphth-2,2'-diolate

Fig. 30.16 Catalyst **41** and substrates **64–67**.

Table 30.12 Hydrogenation of substrates **64–67**. [a)]

Substrate	ee [%]	Conversion [%]	Catalyst	TOF [h^{-1}]
64	92	77	**40**	0.4
65	83	70	**40**	0.1
66	83	87	**40**	0.05
67	94	86	**40**	0.4

a) Hydrogenations carried out in THF at 65 °C using 133 bar H_2 and 5 mol% of **41**.

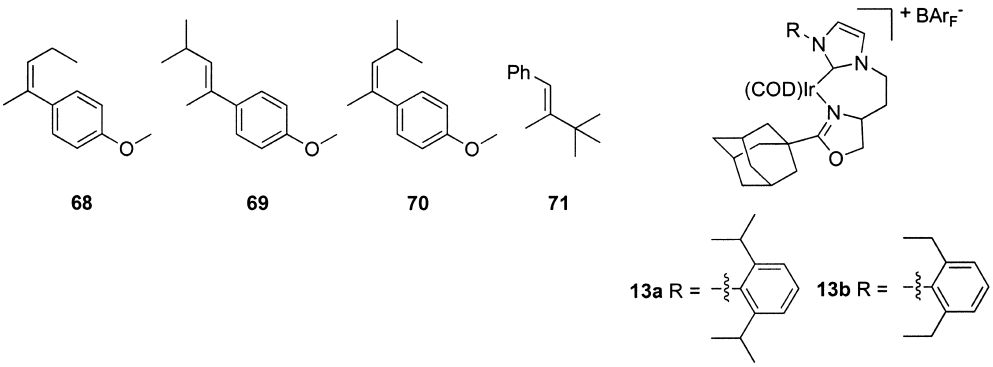

68 **69** **70** **71**

Fig. 30.17 Substrates **68–71** and catalyst **13**.

Table 30.13 Hydrogenation of substrates **68–71** with catalyst **13**.[a)]

Substrate	ee [%]	Conversion [%]	Pressure [bar]	TOF [h^{-1}] (TON)[b)]
68	49	58	50	50
69	97	100	2	80 (167)
70	89	92	2	80
71	86	18	1	15

a) Hydrogenations performed in DCM at 25 °C using 0.6 mol% of catalyst **13**.

a) TON data given where the reaction was complete after a standard reaction time.

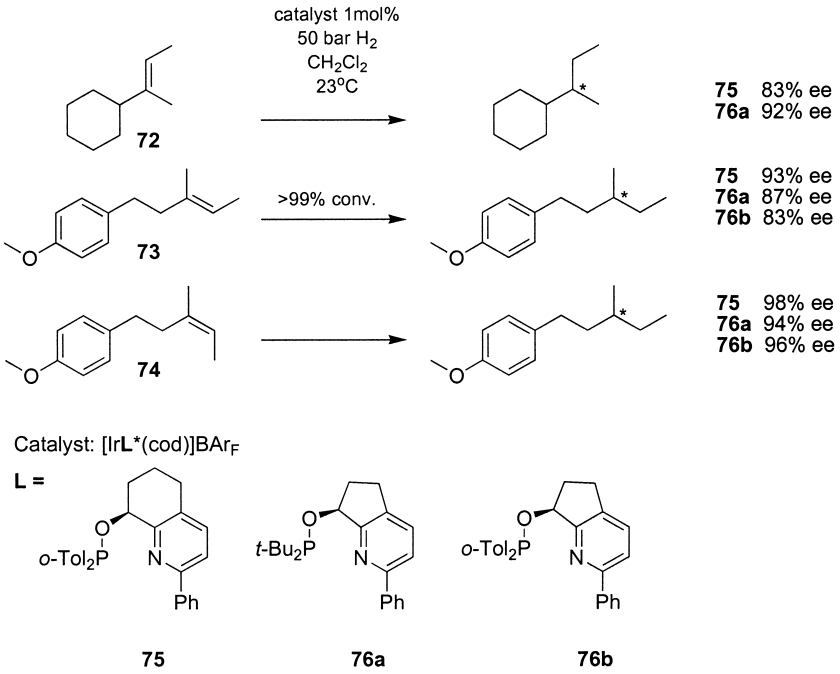

Fig. 30.18 Substrates **72–74** and catalysts **75** and **76**.

30.4 Tetrasubstituted Alkenes

30.4.1 Substrates

Tetrasubstituted alkenes are challenging substrates for enantioselective hydrogenation because of their inherently low reactivity. Crabtree showed that it was possible to hydrogenate unfunctionalized tetrasubstituted alkenes with iridium catalysts [46]. Among the iridium catalysts described in the previous section, several were found to be sufficiently reactive to achieve full conversion with alkene **77** (Table 30.14). However, the enantioselectivities were significantly lower than with trisubstituted olefins, and higher catalyst loadings were necessary.

The highest ee-values were obtained with the PHOX catalyst **42** and the pyridine-derived catalyst **60a** (Table 30.14, entries 1 and 2).

The metallocenes are the most selective catalysts developed to date for the hydrogenation of tetrasubstituted alkenes. However, the required catalyst loadings are relatively high (5–8 mol%). Catalyst **78** was activated with $[PhMe_2NH]^+[(BC_6F_5)_4]^-$ and used to hydrogenate a number of tetrasubstituted alkenes [47] (Fig. 30.20; Table 30.15). The ratios of *cis* to *trans* products obtained from cyclic substrates **80** to **86** were generally high (>95 : 5).

Table 30.14 Enantioselective hydrogenation of **77**.

Entry	Catalyst	Loading [mol%]	Solvent	Temp. [°C]	Pressure [bar]	ee [%]	Absolute config.	TOF [h^{-1}] (TON)[a]	Reference
1	**42c**	2	DCM	r.t.	50	81	–	(50)	29
2	**60a**	1	DCM	r.t.	50	81	–	(100)	44
3	**56b**	1	DCM	r.t.	50	31	*S*	12	18
4	**14b**	1	DCM	r.t.	100	15	*S*	2	26

a) TON data given where no time data were available.

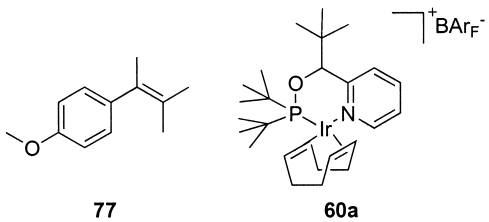

77 **60a**

Fig. 30.19 Substrate **77** and catalyst **60a**.

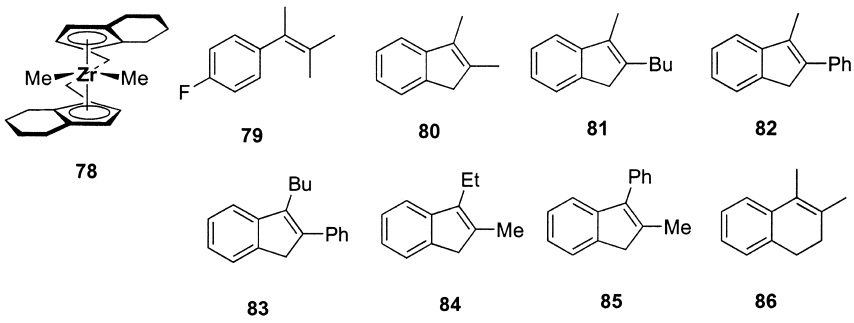

Fig. 30.20 Substrates **79**–**86** and catalyst **78**.

Table 30.15 Hydrogenation of tetrasubstituted alkenes with catalyst **78**. [a)]

Substrate	Absolute configuration	ee [%]	Yield [%]	Pressure [bar]	TON [b)]
79	(+)	96	77	117	10
80	(+)	93	87	117	11
81	(+)	92	96	5	12
82	(–)	99	89	69	18
83	(–)	98	94	103	12
84	–	52	95	117	12
85	(–)	78	94	138	12
86	–	92	91	138	16

a) Hydrogenations performed in benzene at 65 °C using 5–8 mol% catalyst.

b) Reaction times quoted as "between 13 h and 21 h" (30 h for **82**) [47].

30.5 Dienes and Trienes

Burgess and coworkers investigated the hydrogenation of the conjugated diene **87** (Scheme 30.1) [48]. Kinetic studies showed that the reaction occurred mostly stepwise *via* 2,3-diphenyl-1-butene, while only a small part of the diene was converted directly to 2,3-diphenylbutane, without dissociation of the catalyst from the intermediate mono-alkene. The first hydrogenation step was found to proceed with low enantioselectivity, whereas the second step was characterized by strong catalyst and strong substrate control.

In a more recent study [49], a number of similar substrates were hydrogenated. Varying amounts of the *meso* products were detected, and ee-values of 24% to 99% were recorded. With substrates **88**, significant amounts of double bond migration products were formed (Scheme 30.2).

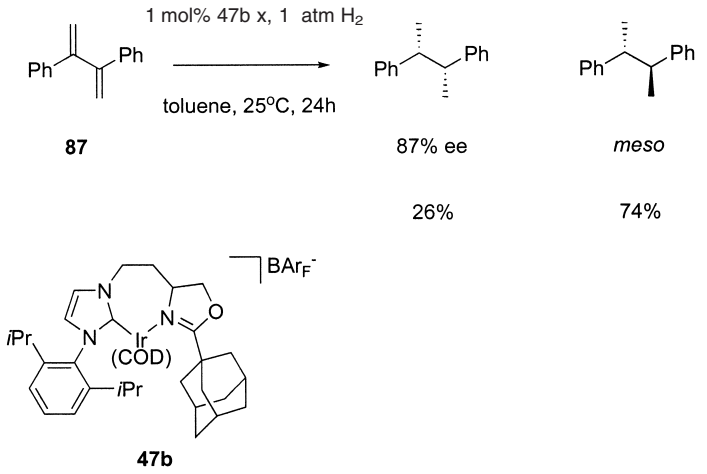

Scheme 30.1 Hydrogenation of substrate **87**.

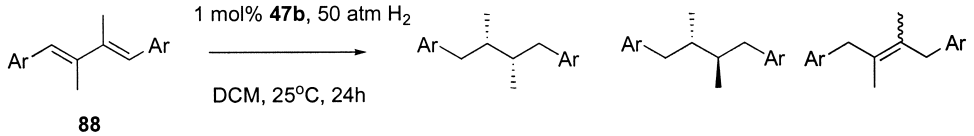

Scheme 30.2 Hydrogenation and double bond migration with dienes **88**.

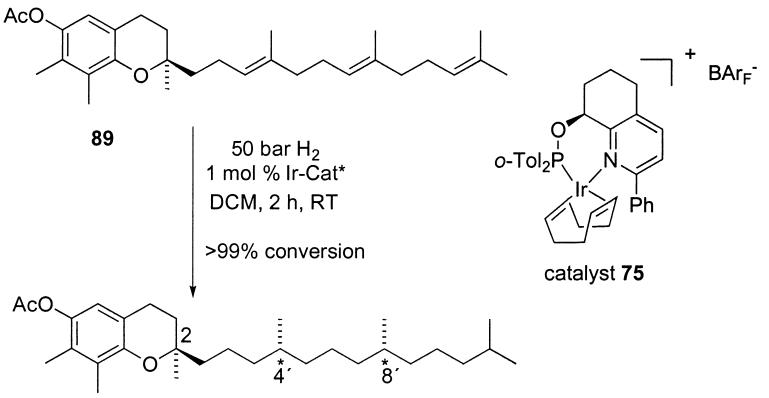

Scheme 30.3 Hydrogenation of vitamin E precursor **89**.

The development of chiral hydrogenation catalysts for unfunctionalized alkenes also allows enantioselective hydrogenation of functionalized olefins where the functionality in the molecule is remote from the double bond. A series of oxazoline-, imidazoline- and pyridine-derived catalysts have been screened for the hydrogenation of unsaturated derivatives of vitamin E (Scheme 30.3). Hy-

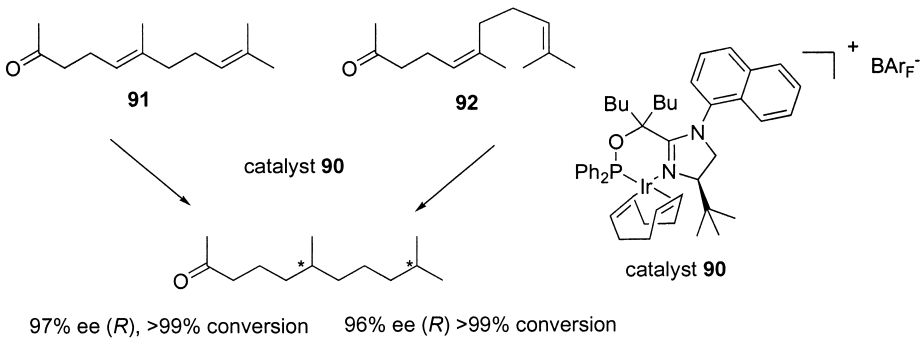

Scheme 30.4 Hydrogenation of dienes **91** and **92**.

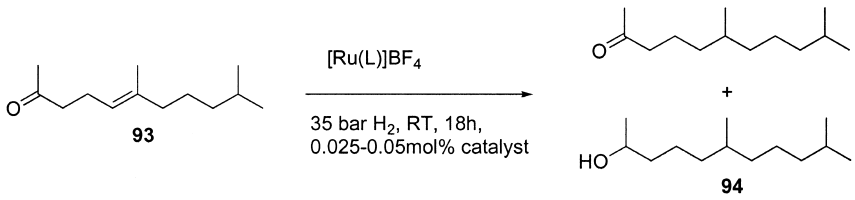

Scheme 30.5 Hydrogenation of substrate **93**.

drogenation of γ-tocotrienyl acetate **89** with catalyst **75** gave the natural (*R,R,R*)-isomer in 98% yield (the remaining 2% being the other three isomers) [50, 51] (Scheme 30.3). Catalyst **90** (Scheme 30.4) was also identified as a very selective catalyst, producing the (*R,R,R*)-isomer with >90% selectivity (<5% *RRS*, <4% *RSR*, <1% *RSS*).

In addition, a number of related dienes and trienes (Scheme 30.4) were hydrogenated with catalyst **90**, with promising results.

Substrate **91** was also hydrogenated in 75% ee using a ruthenium catalyst, [Ru(MeOBIPHEP)](BF$_4$)$_2$ (Scheme 30.4). A similar substrate (**93**, Scheme 30.5) was hydrogenated with a series of ruthenium catalysts: the fully reduced alcohol **94** was a side product. The best result (93% ee, 97:3 ketone:alcohol) was obtained with [Ru(MeOBIPHEP)](BF$_4$)$_2$ [52].

30.6 Conclusions

During recent years, substantial progress has been made in the hydrogenation of unfunctionalized alkenes. With iridium complexes derived from chiral phosphino-oxazolines and related ligands, excellent enantioselectivities and high TON/TOF values can now be obtained for a wide range of unfunctionalized olefins. Most substrates studied to date have at least one aryl substituent at the

double bond. However, recent results (see Section 30.5) have demonstrated that, even for purely alkyl-substituted alkenes, high enantioselectivities can be achieved. Most of the ligands developed so far are modular, allowing optimization of the catalyst structure for a particular substrate.

Tetrasubstituted alkenes remain a challenge. Here, the highest enantioselectivities were obtained with zirconocene catalysts, though the high catalyst loadings required and low TOFs reduce the practicality of these catalysts.

The mechanism of iridium-catalyzed hydrogenation remains unclear. Although several experimental [31, 53, 54] and computational [53, 55, 56] studies have been reported recently, further investigations will be necessary to establish a coherent mechanistic model. Until now, most studies have dealt with simple test substrates; hence, it will be important to explore more complex and also industrially important substrates, in order to determine the full scope and limitations of iridium catalysis.

Abbreviations

DCM	dichloromethane
PHOX	phosphino-oxazoline
r.t.	room temperature
THF	tetrahydrofuran
TOF	turnover frequency
TON	turnover number

References

1 L. Horner, H. Siegel, H. Büthe, *Angew. Chem.* **1968**, 1034.
2 M. Tanaka, I. Ogata, *J. Chem. Soc. Chem. Commun.* **1975**, 735.
3 M. Bianchi, U. Matteoli, P. Frediani, G. Menchi, F. Piacenti, C. Botteghi, M. Marchetti, *J. Organomet. Chem.* **1983**, *252*, 317.
4 K. Inagaki, T. Ohta, K. Nozaki, H. Takaya, *J. Organomet. Chem.* **1997**, *531*, 159.
5 T. Ohta, H. Ikegami, T. Miyake, H. Takaya, *J. Organomet. Chem.* **1995**, *502*, 169.
6 G. S. Forman, T. Ohkuma, W. P. Hems, R. Noyori, *Tetrahedron Lett.* **2000**, *41*, 9471.
7 E. Cesarotti, R. Ugo, H. B. Kagan, *Angew. Chem.* **1979**, *91*, 842.
8 E. Cesarotti, R. Ugo, R. Vitiello, *J. Mol. Catal. Sect. A* **1981**, *12*, 63.
9 L. A. Paquette, J. A. McKinney, M. L. McLaughlin, A. L. Rheingold, *Tetrahedron Lett.* **1986**, *27*, 5599.
10 L. A. Paquette, M. R. Sivik, E. I. Bzowej, K. J. Stanton, *Organometallics* **1995**, *14*, 4865.
11 R. L. Halterman, K. P. C. Vollhardt, M. E. Welker, *J. Am. Chem. Soc.* **1987**, *109*, 8105.
12 V. P. Conticello, L. Brard, M. A. Giardello, Y. Tsuji, M. Sabat, C. L. Stern, T. J. Marks, *J. Am. Chem. Soc.* **1992**, *114*, 2761.
13 C. M. Haar, C. L. Stern, T. J. Marks, *Organometallics* **1996**, *15*, 1765.
14 P. Beagley, P. J. Davies, A. J. Blacker, C. White, *Organometallics* **2002**, *21*, 5852.

15 D. R. Hou, J. H. Reibenspies, T. J. Colacot, K. Burgess, *Chem. Eur. J.* **2001**, *7*, 5391.

16 M. A. Giardello, V. P. Conticello, L. Brard, M. R. Gagné, T. J. Marks, *J. Am. Chem. Soc.* **1994**, *116*, 10241.

17 R. Schmid, E. A. Broger, M. Cereghetti, Y. Crameri, J. Foricher, M. Lalonde, R. K. Müller, M. Scalone, G. Schoettel, U. Zutter, *Pure Appl. Chem.* **1996**, *68*, 131.

18 G. H. Bernardinelli, E. P. Kündig, P. Meier, A. Pfaltz, K. Radkowski, N. Zimmermann, M. Neuburger-Zehnder, *Helv. Chim. Acta* **2001**, *84*, 3233.

19 J. Blankenstein, A. Pfaltz, *Angew. Chem. Int. Ed.* **2001**, *40*, 4445.

20 M. C. Perry, X. Cui, M. T. Powell, D. R. Hou, J. H. Riebenspies, K. Burgess, *J. Am. Chem. Soc.* **2003**, *125*, 113.

21 M. T. Powell, D. R. Hou, M. C. Perry, X. Cui, K. Burgess, *J. Am. Chem. Soc.* **2001**, *123*, 8878.

22 F. Menges, A. Pfaltz, *Adv. Synth. Catal.* **2002**, *344*, 40.

23 T. Focken, G. Raabe, C. Bolm, *Tetrahedron Asymm.* **2004**, *15*, 1693.

24 S. P. Smidt, F. Menges, A. Pfaltz, *Org. Lett.* **2004**, *6*, 2023.

25 S. McIntyre, E. Hörmann, F. Menges, S. P. Smidt, A. Pfaltz, *Adv. Synth. Catal.* **2005**, *347*, 1.

26 K. Källstrom, C. Hedberg, P. Brandt, A. Bayer, P. G. Andersson, *J. Am. Chem. Soc.* **2004**, *126*, 14308.

27 U. Matteoli, V. Beghetto, A. Scrivanti, *J. Mol. Cat. A: Chemical* **1996**, *109*, 45.

28 R. D. Broene, S. L. Buchwald, *J. Am. Chem. Soc.* **1993**, *115*, 12569.

29 A. Lightfoot, P. Schnider, A. Pfaltz, *Angew. Chem. Int. Ed.* **1998**, *37*, 2897.

30 D. G. Blackmond, A. Lightfoot, A. Pfaltz, T. Rosner, P. Schnider, N. Zimmermann, *Chirality* **2000**, *12*, 442.

31 S. Smidt, N. Zimmermann, M. Studer, A. Pfaltz, *Chem. Eur. J.* **2004**, *10*, 4685.

32 A. Pfaltz, J. Blankenstein, R. Hilgraf, E. Hörmann, S. McIntyre, F. Menges, M. Schönleber, S. P. Smidt, B. Wüstenberg, N. Zimmermann, *Adv. Synth. Catal.* **2003**, *345*, 33.

33 Available from Strem: ((4*S*,5*S*)-(–)-*O*-[1-Benzyl-1-(5-methyl-2-phenyl-4,5-dihydrooxazol-4-yl)-2-phenylethyl]-dicyclohexylphosphinite)(1,5-COD)iridium (I) tetrakis(3,5-bis(trifluoromethyl)phenylborate, CAS number 583844-38-6, catalog number 77-5010 and ((4*S*,5*S*)-(+)-*O*-[1-Benzyl-1-(5-methyl-2-phenyl-4,5-dihydrooxazol-4-yl)-2-phenylethyl]-diphenylphosphinite)(1,5-COD)iridium (I) tetrakis(3,5-bis(trifluoromethyl)phenylborate, CAS number 405235-55-4, catalog number 77-5020.

34 R. Hilgraf, A. Pfaltz, *Synlett* **1999**, *11*, 1814.

35 P. Schnider, Ph. D. Dissertation, University of Basel, Basel, **1996**.

36 C. Bolm, T. Focken, G. Raabe, *Tetrahedron Asymm.* **2003**, *14*, 1733.

37 P. G. Cozzi, N. Zimmermann, R. Hilgraf, S. Schaffner, A. Pfaltz, *Adv. Synth. Catal.* **2001**, *343*, 450.

38 P. G. Cozzi, F. Menges, S. Kaiser, *Synlett* **2003**, *6*, 829.

39 W. Tang, W. Wang, X. Zhang, *Angew. Chem. Int. Ed.* **2003**, *42*, 943.

40 G. Xu, S. R. Gilbertson, *Tetrahedron Lett.* **2003**, *44*, 953.

41 D. Liu, W. Tang, X. Zhang, *Org. Lett.* **2004**, *6*, 513.

42 F. Menges, M. Neuburger, A. Pfaltz, *Org. Lett.* **2002**, *4*, 4173.

43 T. Bunlaksananusorn, K. Polborn, P. Knochel, *Angew. Chem.* **2003**, *42*, 3941.

44 W. J. Drury, N. Zimmermann, M. Keenan, M. Hayashi, S. Kaiser, R. Goddard, A. Pfaltz, *Angew. Chem. Int. Ed.* **2004**, *43*, 70.

45 L. B. Schenkel, J. A. Ellman, *J. Org. Chem.* **2003**, *69*, 1800.

46 R. Crabtree, *Acc. Chem. Res.* **1979**, *12*, 331.

47 M. Troutman, D. H. Apella, S. L. Buchwald, *J. Am. Chem. Soc.* **1999**, *121*, 4916.

48 X. Cui, K. Burgess, *J. Am. Chem. Soc.* **2003**, *125*, 14212.

49 X. Cui, J. W. Ogle, K. Burgess, *J. Chem. Soc. Chem. Commun.* **2005**, 672.

50 B. Wüstenberg, Ph. D. Dissertation, University of Basel, Basel, **2003**.

51 S. Bell, B. Wüstenberg, S. Kaiser, F. Menges, T. Netscher, A. Pfaltz, *Science* **2006**, *311*, 642.

52 Patent: EP Appl. 92905551 (1992), USP Appl. 5274125 (1992), E. Broger, J. Foricher, B. Helser, R. Schmid, F. Hoffmann-La Roche AG.

53 C. Mazet, S. P. Smidt, M. Meuwly, A. Pfaltz, *J. Am. Chem. Soc.* **2004**, *126*, 14176.
54 R. Dietiker, P. Chen, *Angew. Chem. Int. Ed.* **2004**, *43*, 5513.
55 P. Brandt, C. Hedberg, P. G. Andersson, *Chem. Eur. J.* **2003**, *9*, 339.
56 Y. Fan, X. Cui, K. Burgess, M. B. Hall, *J. Am. Chem. Soc.* **2004**, *126*, 16688.